Longitudinal interlayer magnetoresistance in strongly anisotropic quasi-two-dimensional metals

P. D. Grigoriev*
L. D. Landau Institute for Theoretical Physics, Chernogolovka, Russia
(Received 15 March 2013; revised manuscript received 23 July 2013; published 19 August 2013)

In strongly anisotropic quasi-two-dimensional (2D) metals, where the interlayer band width is less than the Landau level separation, the role of impurity scattering is enhanced by a magnetic field perpendicular to the conducting layers. This leads to a longitudinal magnetoresistance (MR) in contrast to the prediction of classical theory based on the constant-τ approximation. The MR has a square-root dependence $R_{zz}(B_z)$ in a strong field, being linear in the intermediate region. The crossover field allows to estimate the interlayer transfer integral or electron mean-free time. Longitudinal interlayer MR, being robust to the increase of temperature or long-range disorder, is easy for measurements and provides a useful tool to investigate the electronic structure of quasi-2D compounds.

DOI: 10.1103/PhysRevB.88.054415 PACS number(s): 74.72.−h, 72.15.Gd, 73.43.Qt, 74.70.Kn

The investigation of the angular and field dependence of magnetoresistance (MR) is a powerful tool to study the electronic properties of various metals, including strongly anisotropic layered compounds, such as organic metals (see, e.g., Refs. 1–4 for reviews), cuprate and iron-based high-temperature superconductors (see, e.g., Refs. 5–14), heterostructures,[15] and so on. In layered quasi-two-dimensional (Q2D) metals with at least monoclinic crystal symmetry the electron dispersion in the tight-binding approximation is given by

$$\epsilon_{3D}(\mathbf{k}) \approx \epsilon_{2D} - 2t_z \cos(k_z d), \tag{1}$$

where the 2D electron dispersion in magnetic field B perpendicular to conducting layers is quantized in Landau levels:

$$\epsilon_{2D} = \epsilon_{2D}(n) = \hbar\omega_c(n+\gamma). \tag{2}$$

Here the Landau level (LL) separation $\hbar\omega_c = \hbar eB/m^*c$, e is the electron charge, $\hbar$ is the Planck's constant, m^* is the effective electron mass, n is the LL number, γ is the Onsager phase equal to $1/2$ usually, k_z is out-of-plane electron momentum, and d is the interlayer spacing. If the interlayer transfer integral $t_z \gg \hbar\omega_c$, the standard three-dimensional (3D) theory of galvanomagnetic properties based on kinetic equation in the τ approximation can be applied,[16–18] which is valid in the lowest order in the parameter $\hbar\omega_c/t_z$. This theory predicts several peculiarities of MR in Q2D metals: the angular magnetoresistance oscillations (AMRO)[19–21] and the beats of the amplitude of magnetic quantum oscillations (MQO).[17]

In more anisotropic Q2D metals, when $t_z \gtrsim \hbar\omega_c$, some new features appear, such as slow MR oscillations[22,23] and the phase shift of MQO beats between transport and thermodynamic quantities.[23,24] These two effects are not described by the standard 3D theory[16–18] because they appear in the higher orders in the parameter $\hbar\omega_c/t_z$. The monotonic part of MR also changes when $\hbar\omega_c/t_z \sim 1$. According to the standard theory,[16] the external magnetic field along the electric current leads only to MQO but does not influence the monotonic (background) part of this current.[25] However, the monotonic growth of interlayer MR R_{zz} with the increase of longitudinal magnetic field B_z was observed in various compounds as a general feature of Q2D metals.[22,26–33]

In very anisotropic compounds with $t_z \ll \Gamma_0, \hbar\omega_c$, where $\Gamma_0 = \hbar/2\tau_0$ and τ_0 is electron mean free time in the absence of magnetic field, this monotonic growth of $R_{zz}(B_z)$ becomes stronger.[26–33] First, it was attributed to additional "strongly incoherent" mechanisms of interlayer electron transport, which do not conserve the in-plane electron momentum during interlayer electron hopping: the interlayer hopping via local crystal defects with in-series intralayer metallic transport,[31] or the metal-insulator transition and variable-range electron hopping.[34] The transverse interlayer MR in the "strongly incoherent" regime is weaker than in the coherent 3D theory.[31,35,36] However, in most experiments the interlayer MR shows the pronounced AMRO and metallic-type temperature dependence, which is incompatible with the "strongly incoherent" mechanisms.

Recently it was shown[37–40] that at very weak interlayer coupling $t_z \ll \Gamma_0 \ll \hbar\omega_c$, the longitudinal interlayer magnetoresistance has a square-root monotonic growth $R_{zz} \propto \sqrt{B_z}$ even within the coherent-tunnelling model and one-particle approximation.[41] The angular dependence of MR also changes in this limit,[37] which contradicts the previous common opinion[42] that in the "weakly incoherent" regime, i.e., at $\Gamma_0 > t_z$, the interlayer magnetoresistance does not differ from the coherent 3D limit with $t_z \gg \Gamma_0$. However, the limitation $t_z \ll \Gamma_0 \ll \hbar\omega_c$ of this calculation[37–39] is very restrictive. In the present paper we calculate the longitudinal interlayer magnetoresistance at $\Gamma_0 \lesssim 4t_z < \hbar\omega_c$ using another approach, based on the strongly anisotropic 3D electron dispersion in Eq. (1). This extends the study in Refs. 37–39 to finite $t_z \gtrsim \Gamma_0$ and helps to understand the relation between these two approaches.

At $t_z \gtrsim \Gamma_0$ one can start from the 3D electron dispersion (1), considering impurity scattering as a perturbation. Below we show that if the perturbation theory is applicable, this approach gives a correct result even at $t_z < \Gamma_0$. The interlayer electron conductivity can be evaluated at finite temperature using the 3D Kubo formula,[43–45] which gives

$$\sigma_{zz} = \int d\varepsilon[-n_F'(\varepsilon)]\,\sigma_{zz}(\varepsilon), \tag{3}$$

where the derivative of the Fermi distribution function $n_F'(\varepsilon) = -1/\{4T\cosh^2[(\varepsilon-\mu)/2T]\}$, and the zero-temperature

conductivity at energy ε is

$$\sigma_{zz}(\varepsilon) = \frac{e^2\hbar}{2\pi}\sum_m v_z^2(k_z)[2\mathrm{Im}G_R(m,\varepsilon)]^2\,, \tag{4}$$

where $v_z = \partial\epsilon_{3D}/\partial k_z = 2t_z d\sin(k_z d)/\hbar$ is the interlayer electron velocity, the sum over the electron quantum numbers $m \equiv \{n,k_y,k_z\}$ (excluding spin) is taken in the unit volume, and the retarded electron Green's function

$$G_R = [\varepsilon - \epsilon_{3D}(m) - \Sigma^R(\varepsilon,m)]^{-1}. \tag{5}$$

In the self-consistent Born approximation (SCBA) and even in the "noncrossing" approximation the electron self-energy $\Sigma^R(\varepsilon,m) = \Sigma_n^R(\varepsilon)$ is independent of k_y and k_z [see Refs. 23,46–48 or Eqs. (11) to (14) below]. Since $\epsilon_{3D}(m)$ is also independent of k_y, the summation over k_y in Eq. (4) gives the factor equal to the LL degeneracy of one conducting layer per spin state $N_{LL} = 1/2\pi l_H^2 = eB_z/2\pi\hbar c$ (Refs. 49). The interlayer conductivity is now given by a sum over LLs

$$\sigma_{zz}(\varepsilon) = \sum_n \sigma_n(\varepsilon)\,, \tag{6}$$

where the contribution to σ_{zz} from the nth LL is

$$\sigma_n = \frac{e^2\hbar N_{LL}}{2\pi}\int\frac{dk_z}{2\pi}v_z^2(k_z)[2\mathrm{Im}G_R(n,k_z,\varepsilon)]^2\,. \tag{7}$$

Substituting Eq. (5) and performing the integration over k_z in Eq. (7), one obtains

$$\sigma_n = \frac{\sigma_0\hbar\omega_c\Gamma_0}{2\pi t_z^2\left|\mathrm{Im}\Sigma_n^R(\varepsilon)\right|}\,\mathrm{Re}\frac{4t_z^2 - (\Delta\varepsilon)^2 + i\,\Delta\varepsilon\left|\mathrm{Im}\Sigma_n^R(\varepsilon)\right|}{\sqrt{4t_z^2 - \left(\Delta\varepsilon - i\,\left|\mathrm{Im}\Sigma_n^R(\varepsilon)\right|\right)^2}}, \tag{8}$$

where $\Delta\varepsilon \equiv \varepsilon - \epsilon_{2D}(n) - \mathrm{Re}\Sigma_n^R(\varepsilon)$, and σ_0 denotes the interlayer conductivity without magnetic field:

$$\sigma_0 = e^2\rho_F\left\langle v_z^2\right\rangle\tau_0 = 2e^2N_{LL}t_z^2 d/\hbar^2\omega_c\Gamma_0, \tag{9}$$

$\rho_F = 2N_{LL}/\hbar\omega_c d = m^*/\pi\hbar^2 d$ is the 3D density of states (DoS) at the Fermi level in the absence of magnetic field per two spin components $\tau_0 = \hbar/2\Gamma_0$ and $\langle v_z^2\rangle = 2t_z^2 d^2/\hbar^2$.

The expansion of Eq. (8) up to the first-order term in t_z^2 gives

$$\sigma_n = \frac{2\sigma_0\hbar\omega_c\Gamma_0\left|\mathrm{Im}\,\Sigma_n^R(\varepsilon)\right|^2}{\pi\left[(\Delta\varepsilon)^2 + \left|\mathrm{Im}\Sigma_n^R(\varepsilon)\right|^2\right]^2}, \tag{10}$$

which coincides[50] with Eq. (32) of Ref. 37 or with Eq. (14) of Ref. 38. This shows the equivalence of two approaches at $t_z < \Gamma_0$ to calculate conductivity, namely using the the 3D anisotropic dispersion (1) and using the tunneling between only two adjacent 2D conducting layers as in Refs. 37,38. Previously this equivalence was shown only for AMRO without MQO.[42,51]

How general is this equivalence? Both approaches are based on the perturbation theory for the stack of isolated 2D electron layers with two perturbations: the impurity potential and the finite interlayer hopping. These two approaches differ by the sequence, in which the above two perturbations are taken into account. If the same subset of diagrams (the terms in the perturbation series) is calculated in different orders, the result is the same. But the changing of the sequence may result in the summation of different subsets of diagrams, e.g., to give higher-order terms in the perturbation which is considered first. Moreover, the perturbation theory itself is often not applicable, as, e.g., in a metal-insulator transition. Then the sequence of taking different perturbations into account is important and can lead to physically different predictions. Equation (10) only proves the equivalence of two-layer and 3D-dispersion approaches for the interlayer conductivity calculation in the second order in the interlayer transfer integral t_z within the one-particle approximation and with sufficiently weak disorder (i.e., far from any metal-insulator transition). Since both approaches correspond to the summation of the same subset of diagrams for the interlayer magnetoresistance, at $2t_z \lesssim \Gamma_0$ for the described model both approaches are valid. The anisotropic-dispersion approach may be inapplicable only at very small t_z, when the 2D weak-localization corrections appear,[52] or when the Coulomb blockade of interlayer electron transport becomes important.[53,54] The two-layer approach becomes inapplicable at large $t_z \gtrsim \sqrt{\Gamma_0\hbar\omega_c}$, when the nonlinear terms in t_z^2 become important, as one can see from Eq. (8) and from Figs. 1 and 2 below.

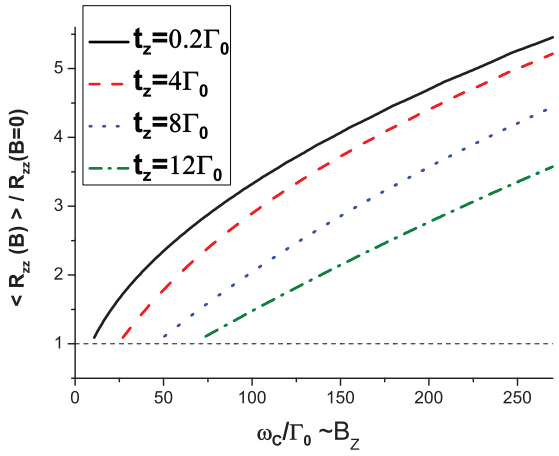

FIG. 1. (Color online) Average interlayer magnetoresistance $\bar{R}_{zz}(B_z) = 1/\bar{\sigma}_{zz}$ as a function of magnetic field B_z/Γ_0, calculated at $4t_z < \hbar\omega_c$ using Eqs. (8) and (16) at four different values of $t_z/\Gamma_0 = 0.2$ (solid black line), $t_z/\Gamma_0 = 4$ (dashed red line), $t_z/\Gamma_0 = 8$ (dotted blue line), and $t_z/\Gamma_0 = 12$ (dash-dotted green line). At $t_z \gg \Gamma_0$ there is a wide interval $4t_z < \hbar\omega_c \ll (4t_z)^2/\Gamma_0$ of linear MR (see dash-dotted green line), while at smaller t_z MR has a square-root field dependence $\bar{R}_{zz}(B_z) \propto \sqrt{B_z}$ (solid black and dashed red lines).

To calculate the electron self-energy $\Sigma_n^R(\varepsilon)$ entering Eq. (8) we apply the standard model of 3D strongly anisotropic metals with short-range disorder. The Hamiltonian consists of two terms: $\hat{H} = \hat{H}_0 + \hat{H}_I$. The first term $\hat{H}_0 = \sum_m \epsilon_{3D}(m)\,c_m^+ c_m$ describes the 3D noninteracting electrons in a magnetic field with the anisotropic dispersion given by Eqs. (1) and (2). The second term $\hat{H}_I = \sum_i V_i(r)\,\Psi^+(r)\,\Psi(r)$ describes the electron interaction with impurities. The impurities are taken to be point-like with the potential $V_i(r) = U\delta^3(r - r_i)$ and randomly distributed with volume concentration n_i. Without magnetic field the broadening $\Gamma_0 = |\mathrm{Im}\Sigma|$ of the electron levels due to the scattering by impurities in the Born approximation is $\Gamma_0 \approx \pi n_i U^2\rho_F/2$. In Q2D metals in a strong

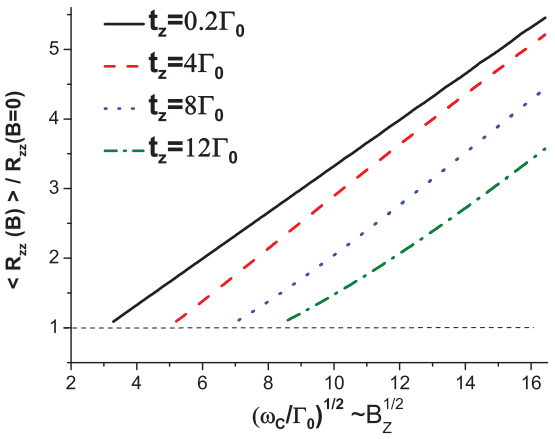

FIG. 2. (Color online) The same as in Fig. 1 but as function of the square root of the magnetic field. At $t_z \lesssim \Gamma_0$ MR $\bar{R}_{zz}(B_z) \propto \sqrt{B_z}$ (solid black and dashed red curves are linear). At larger $t_z \gg \Gamma_0$ this dependence transforms to linear MR $\bar{R}_{zz}(B_z) \propto B_z$ (see dotted blue and dash-dotted green lines, which look like parabolas).

magnetic field $\hbar\omega_c > 4t_z, \Gamma_0$, the electron self-energy Σ_n^R depends on the energy deviation $\Delta\epsilon$ from the nth LL. In the "noncrossing" or "single-site" approximation,[55–57] which includes all diagrams without the intersection of impurity lines, the electron Green's function averaged over impurity configurations has the form (see the Appendix of Ref. 37)

$$G(\boldsymbol{r}_1,\boldsymbol{r}_2,\varepsilon) = \sum_{n,k_y,k_z} \frac{\Psi^{0*}_{n,k_y,k_z}(\boldsymbol{r}_1)\Psi^{0}_{n,k_y,k_z}(\boldsymbol{r}_2)}{\varepsilon - \epsilon_{3D}(n,k_z) - \Sigma_n(\varepsilon)}, \tag{11}$$

where $\Psi^0_{n,k_y,k_z}(\boldsymbol{r})$ are the electron wave functions in a magnetic field without impurities and $\Sigma_n(\varepsilon)$ is the electron self-energy, averaged over impurity positions and given by the equation

$$\Sigma_n(\varepsilon) = n_i U / [1 - UG(\varepsilon)]. \tag{12}$$

$G(\varepsilon) \equiv G(\boldsymbol{r},\boldsymbol{r},\varepsilon)$ after the integration over k_y and k_z becomes

$$G(\varepsilon) = \sum_n \frac{N_{LL}/d}{\sqrt{(\varepsilon - \epsilon_{2D}(n) - \Sigma_n(\varepsilon))^2 - 4t_z^2}}. \tag{13}$$

The system of equations (12) and (13) allows to calculate the electron self-energy $\Sigma_n(\varepsilon)$ numerically.

For the weak impurity potential $UG(\varepsilon) \sim U\rho_F \ll 1$ the self-consistent Born approximation (SCBA) is applicable, and Eq. (12) reduces to

$$\Sigma(\varepsilon) \approx n_i U + n_i U^2 G(\varepsilon). \tag{14}$$

The SCBA is valid when the scattering potential of each impurity is weak compared to the Fermi energy E_F, but the concentration of impurities n_i can be arbitrary,[58] so that Γ_0 is also arbitrary. It can be shown by the method of Ref. 38 that one needs at least SCBA to obtain a qualitatively correct monotonic growth of interlayer longitudinal MR, which differs in SCBA and in the noncrossing approximations only by a factor of 4/3. The similar system of SCBA equations for the electron Green's function in Q2D metals in a magnetic field was written previously,[23,46–48] but the interlayer conductivity was calculated only in the simple Born approximation there. In Refs. 23,46 only the limit $2\pi t_z \gg \hbar\omega_c$ has been considered, while in Ref. 47 a large electron reservoir was introduced to damp the MQO of the chemical potential[44] and to make the simple Born approximation applicable.

In the strong magnetic field limit, when $\hbar\omega_c/4 > t_z, \Gamma_0$ and the LLs do not overlap, we can consider only one LL in the solution of SCBA equations (13) and (14), which simplify to

$$\Sigma_* = \frac{n_i U^2 N_{LL}/d}{\sqrt{(\Delta\epsilon - \Sigma_*)^2 - 4t_z^2}} = \frac{\Gamma_0 \hbar\omega_c/\pi}{\sqrt{(\Delta\epsilon - \Sigma_*)^2 - 4t_z^2}}, \tag{15}$$

where $\Sigma_* \equiv \Sigma_n(\varepsilon) - n_i U$ and $\Delta\epsilon \equiv \varepsilon - \epsilon_{2D}(n) - n_i U = \Delta\varepsilon + \mathrm{Re}\Sigma_*$. At $t_z = 0$ one obtains the 2D result[59] for the electron self-energy in SCBA. Note that the impurity scattering enters Eq. (15) only in the combination $n_i U^2 N_{LL}/d = \Gamma_0\hbar\omega_c/\pi \equiv \Gamma_*^2$. Therefore, at $\hbar\omega_c/4 > t_z, \Gamma_0$, $\Gamma_* \equiv \sqrt{\Gamma_0\hbar\omega_c/\pi}$ is the only energy scale in Eq. (15), and $|\mathrm{Im}\Sigma_*| \sim \Gamma_* \propto \sqrt{B_z}$ in agreement with Refs. 55,59, which leads to the same field dependence of background MR:[37,38] $R_{zz} \approx R_{zz0}\,|\mathrm{Im}\Sigma(\mu,B)|/\Gamma_0 \propto \sqrt{B_z}$. Equation (15) rewrites as the fourth-order algebraic equation:

$$\Sigma_*^2\left[(\Delta\epsilon - \Sigma_*)^2 - 4t_z^2\right] = \Gamma_*^4. \tag{16}$$

Among four solutions of this equation, only one satisfies the physical requirement $\Sigma_* \to 0$ at $\Delta\epsilon \to \pm\infty$. This solution gives $\mathrm{Im}\Sigma_* \neq 0$ in the finite energy interval of the width $\sim 4\sqrt{\Gamma_*^2 + t_z^2}$, while $\mathrm{Re}\Sigma_n$ has cusps at the boundaries of this interval. Now we substitute the physical solution of Eq. (16) into Eq. (8). In the calculation of conductivity in 3D metals one usually omits the real part $\mathrm{Re}\Sigma$ of the electron self-energy. However, in quasi-2D metals in high magnetic field $\mathrm{Re}\Sigma$ must be taken into account because it strongly depends on energy. If one neglects $\mathrm{Re}\Sigma_n$ in Eq. (8), the shape of the curves in Fig. 1 modifies.

The result for the monotonic part of interlayer MR $\langle R_{zz}\rangle = 1/\bar{\sigma}_{zz}$ is shown in Figs. 1 and 2, where $\bar{\sigma}_{zz}$ is the conductivity averaged over period $\hbar\omega_c$ of MQO. From Fig. 1 we see the crossover from linear to square-root field dependence of interlayer background MR $R_{zz}(B_z)$: the lowest curve, corresponding to $t_z = 12\Gamma_0$, is almost linear, while the curves at smaller t_z have almost square-root field dependence. The interval of the linear MR is $4t_z < \hbar\omega_c \ll (4t_z)^2/\Gamma_0$ and increases with the increase of t_z/Γ_0. All curves at $B_z = 0$ must come to 1, which enlarges the region of linear MR as compared to Figs. 1 and 2. However, the above calculation is applicable only in a strong field, $\hbar\omega_c/4 > t_z, \Gamma_*$. The crossover from linear to square-root dependence of MR is a general feature of quasi-2D metals and already has been observed in a number of experiments (see, e.g., Refs. 26,27). The square-root dependence $R_{zz} \propto B_z$ is now obtained at $\hbar\omega_c > 2\Gamma_* \gtrsim 4t_z$, i.e., in a much wider region than the limitation $\hbar\omega_c \gg \Gamma_0 \gg t_z$ of the calculation in Refs. 37,38.

This field dependence of interlayer MR can be understood as follows. Equation (16) simplifies to a quadratic equation at $\Delta\epsilon = 0$ and has two solutions: $\Sigma_*^2 = 2t_z^2 \pm \sqrt{4t_z^4 + \Gamma_*^4}$. The physical solution does not diverge at $t_z \to \infty$, has a nonzero imaginary part, and at $t_z = 0$ agrees with the 2D limit described by T. Ando in Refs. 55,59. All these criteria are satisfied for

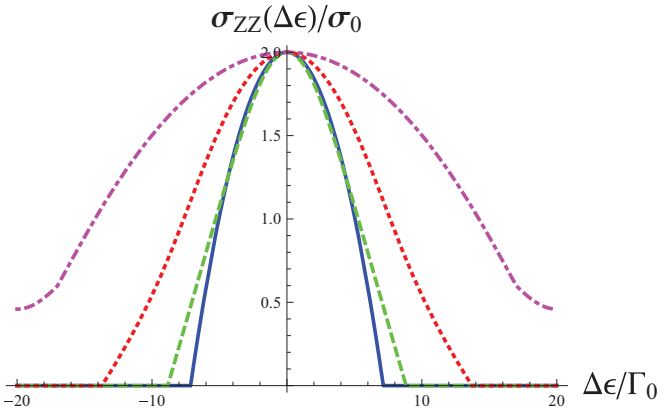

FIG. 3. (Color online) Interlayer conductivity $\sigma_{zz}(\Delta\epsilon)$ calculated from Eqs. (8) and (16) in the strong-field limit $\hbar\omega_c/\Gamma_0 = 40$ as a function of energy counted from the nearest LL at four different values of $t_z/\Gamma_0 = 0.1$ (solid blue line), $t_z/\Gamma_0 = 2$ (dashed green line), $t_z/\Gamma_0 = 5$ (dotted red line), and $t_z/\Gamma_0 = 10$ (dash-dotted magenta line). In the limit $2t_z^2 \gg \Gamma_0\hbar\omega_c$ the interlayer conductivity has approximately a semicircle shape of width $2t_z$. In the opposite limit $\Gamma_0\hbar\omega_c \gg t_z^2$ the "conducting band" of each LL has the width $\sim\sqrt{\Gamma_0\hbar\omega_c}$.

sign "−," which at $\Delta\epsilon = 0$ gives Re $\Sigma_* = 0$ and

$$|\mathrm{Im}\Sigma_*| = \sqrt{\sqrt{4t_z^4 + \Gamma_*^4} - 2t_z^2}. \tag{17}$$

Substituting this to Eq. (8) one obtains

$$\sigma_n(\Delta\epsilon = 0) = \frac{2\sigma_0\hbar\omega_c\Gamma_0}{\pi\Gamma_*^2} = 2\sigma_0. \tag{18}$$

Thus, in the minima of MQO, the interlayer MR may drop to the values not smaller than $R_{zz}(B = 0)/2$. In the limit $\hbar\omega_c > 4t_z \gg \sqrt{\Gamma_0\hbar\omega_c}$ each LL gives an essential contribution to conductivity in the interval $-2t_z \lesssim \Delta\epsilon \lesssim 2t_z$. This follows from Eq. (16) and can be seen from Fig. 3, where the conductivity as a function of energy distance $\Delta\epsilon$ to the nearest LL has a dome shape of the width $W \approx 4t_z$, coinciding with the bandwidth along the z axis in the absence of disorder. The conductivity, averaged over period $\hbar\omega_c$ of MQO, is then given by

$$\bar{\sigma}_{zz} = \int_{-\hbar\omega_c/2}^{\hbar\omega_c/2} \frac{d\varepsilon}{\hbar\omega_c}\sigma_{zz}(\Delta\epsilon) \approx \sigma_{zz}(0)\,\frac{\pi}{4}\,\frac{W}{\hbar\omega_c}$$
$$= \sigma_0(2\pi t_z/\hbar\omega_c) \propto 1/B_z. \tag{19}$$

This predicts a linear background magnetoresistance $R_{zz} = 1/\bar{\sigma}_{zz} \propto B_z$ in the interval $4t_z < \hbar\omega_c \ll (4t_z)^2/\Gamma_0$ of the magnetic field in quasi-2D strongly anisotropic compounds. Equation (19) also predicts a stronger dependence of $\bar{\sigma}_{zz}$ on t_z: $\bar{\sigma}_{zz} \propto t_z^3$, unlike the usual dependence $\bar{\sigma}_{zz} \approx \sigma_0 \propto t_z^2$. In Figs. 1 and 2 this unusual t_z dependence reveals in the decrease of $\langle R_{zz}\rangle/R_{zz0} = \sigma_0/\bar{\sigma}_{zz}$ at the same $\hbar\omega_c/\Gamma_0$ with the increase of t_z. The obtained nonquadratic dependence $\bar{\sigma}_{zz} \propto t_z^3$ also means that the two-layer approach becomes inapplicable at $t_z \gtrsim \Gamma_* = \sqrt{\Gamma_0\hbar\omega_c/\pi}$.

In the opposite limit $\hbar\omega_c \gg \Gamma_* \gtrsim t_z$ the "width of the conducting band" from each LL is $W \approx 4\Gamma_*$, and for the background interlayer conductivity one obtains $\bar{\sigma}_{zz}/\sigma_0 \approx 2\sqrt{\Gamma_0/\hbar\omega_c} \propto 1/\sqrt{B_z}$, or

$$\bar{R}_{zz}(B)/\bar{R}_{zz}(0) \approx \sqrt{\hbar\omega_c/4\Gamma_0} \propto \sqrt{B_z} \tag{20}$$

in agreement with Refs. 37–40 and Fig. 2.

The magnetic field B_{cr} of the crossover from linear to square-root dependence of MR $R_{zz}(B_z)$ can be used to estimate the value of the interlayer transfer integral in the compound: $t_z \sim \sqrt{\Gamma_0\hbar\omega_c}$, where $\omega_c = eB_{\mathrm{cr}}/m^*c$ corresponds to the crossover field. However, distinguishing linear from square-root MR dependence requires a large interval of the magnetic field. In Fig. 2 this crossover field can be seen on the dotted blue curve at $\sqrt{\hbar\omega_c/\Gamma_0} \approx 11$. This crossover also appears on the dash-dotted green curve at $\sqrt{\hbar\omega_c/\Gamma_0} \approx 15$.

The obtained monotonic growth of MR originates from MQO but survives at a much higher temperature, when MQO are completely suppressed. According to Eqs. (3) and (4), the temperature smearing of the Fermi distribution function does not influence the monotonic dependence of MR. Only at much higher temperature, when the electron scattering by phonons plays a major role in the relaxation of electron momentum, the above monotonic dependence of MR is weakened. Similarly, the long-range disorder, not included in the above calculation, produces the local variation of the Fermi energy along the sample on the scale greater than the magnetic length, which damps the MQO but keeps the monotonic part of MR almost unchanged. Therefore, even if MQO are not seen in a compound because of strong disorder or high temperature, the background longitudinal interlayer MR can be observed and provides useful information about the electronic structure of this compound. This feature of the background MR is similar to that of slow oscillations in Q2D compounds at $t_z > \hbar\omega_c$ (Ref. 22).

To summarize, the calculation of longitudinal interlayer magnetoresistance in Q2D metals is performed in the strong-field limit $\hbar\omega_c > 4t_z$ based on the anisotropic 3D electron dispersion. It predicts a linear background MR $\bar{R}_{zz}(B_z) = 1/\bar{\sigma}_{zz} \propto B_z$ in the interval $4t_z < \hbar\omega_c \ll (4t_z)^2/\Gamma_0$ of magnetic field, where $\bar{\sigma}_{zz}$ has also unusual dependence on the interlayer transfer integral: $\bar{\sigma}_{zz} \propto t_z^3$. At stronger field or at smaller $t_z < \sqrt{\Gamma_0\hbar\omega_c}$, the usual dependence $\bar{\sigma}_{zz} \propto t_z^2$ is recovered, and the MR transforms to the square-root dependence $R_{zz}(B_z) \propto \sqrt{B_z}$, as was recently obtained in the limit $t_z \ll \Gamma_0 \ll \hbar\omega_c$ using the two-layer tunneling approach.[37–39] The present calculation extends these results to the region $\sqrt{\Gamma_0\hbar\omega_c} \gtrsim t_z \gtrsim \Gamma_0$, but shows that at $t_z \gtrsim \sqrt{\Gamma_0\hbar\omega_c}$ the MR behavior changes and the two-layer tunneling approach becomes inapplicable. The magnetic field of the crossover from the linear to square-root dependence of $\bar{R}_{zz}(B_z)$ allows to estimate the interlayer transfer integral $t_z \sim \sqrt{\Gamma_0\hbar\omega_c}$ from the experimental data. The obtained longitudinal MR $\bar{R}_{zz}(B_z)$ helps to explain numerous experiments on interlayer MR in strongly anisotropic quasi-2D compounds.[22,26–33] The measurement of the monotonic part of longitudinal interlayer MR is much easier than the measurement of MQO or AMRO because a finite temperature and long-range crystal imperfections do not affect $\bar{R}_{zz}(B_z)$ up to much higher temperatures or disorder. Therefore, the experimental study of longitudinal interlayer background magnetoresistance is proposed as a simple additional tool

to investigate the electronic structure of strongly anisotropic quasi-two-dimensional compounds in a wide range of parameters.

The work was supported by RFBR, by SIMTECH Program (Grant No. 246937) and by NEXT Program (No. 11 LABX 075).

*grigorev@itp.ac.ru

[1] J. Wosnitza, *Fermi Surfaces of Low-Dimensional Organic Metals and Superconductors* (Springer-Verlag, Berlin, 1996); J. Singleton, Rep. Prog. Phys. **63**, 1111 (2000).

[2] T. Ishiguro, K. Yamaji, and G. Saito, *Organic Superconductors*, 2nd Ed., (Springer-Verlag, Berlin, 1998).

[3] M. V. Kartsovnik, Chem. Rev. **104**, 5737 (2004).

[4] M. V. Kartsovník and V. G. Peschansky, Fiz. Nizk. Temp. **31**, 249 (2005) [Low Temp. Phys. **31**, 185 (2005)].

[5] N. E. Hussey, M. Abdel-Jawad, A. Carrington, A. P. Mackenzie, and L. Balicas, Nature (London) **425**, 814 (2003).

[6] M. Abdel-Jawad, M. P. Kennett, L. Balicas, A. Carrington, A. P. Mackenzie, R. H. McKenzie, and N. E. Hussey, Nat. Phys. **2**, 821 (2006).

[7] Nicolas Doiron-Leyraud, Cyril Proust, David LeBoeuf, Julien Levallois, Jean-Baptiste Bonnemaison, Ruixing Liang, D. A. Bonn, W. N. Hardy, and Louis Taillefer, Nature (London) **447**, 565 (2007).

[8] M. Abdel-Jawad, J. G. Analytis, L. Balicas, A. Carrington, J. P. H. Charmant, M. M. J. French, and N. E. Hussey, Phys. Rev. Lett. **99**, 107002 (2007).

[9] Malcolm P. Kennett and Ross H. McKenzie, Phys. Rev. B **76**, 054515 (2007).

[10] B. Vignolle, A. Carrington, R. A. Cooper, M. M. J. French, A. P. Mackenzie, C. Jaudet, D. Vignolles, Cyril Proust, and N. E. Hussey, Nature (London) **455**, 952 (2008).

[11] T. Helm, M. V. Kartsovnik, M. Bartkowiak, N. Bittner, M. Lambacher, A. Erb, J. Wosnitza, and R. Gross, Phys. Rev. Lett. **103**, 157002 (2009).

[12] T. Helm, M. V. Kartsovnik, I. Sheikin, M. Bartkowiak, F. Wolff-Fabris, N. Bittner, W. Biberacher, M. Lambacher, A. Erb, J. Wosnitza, and R. Gross, Phys. Rev. Lett. **105**, 247002 (2010).

[13] Taichi Terashima, Nobuyuki Kurita, Megumi Tomita, Kunihiro Kihou, Chul-Ho Lee, Yasuhide Tomioka, Toshimitsu Ito, Akira Iyo, Hiroshi Eisaki, Tian Liang, Masamichi Nakajima, Shigeyuki Ishida, Shin-ichi Uchida, Hisatomo Harima, and Shinya Uji, Phys. Rev. Lett. **107**, 176402 (2011).

[14] D. Graf, R. Stillwell, T. P. Murphy, J.-H. Park, E. C. Palm, P. Schlottmann, R. D. McDonald, J. G. Analytis, I. R. Fisher, and S. W. Tozer, Phys. Rev. B **85**, 134503 (2012).

[15] M. Kuraguchi, E. Ohmichi, T. Osada, and Y. Shiraki, Synth. Met. **133-134**, 113 (2003).

[16] A. A. Abrikosov, *Fundamentals of the Theory of Metals* (North-Holland, Amsterdam, 1988).

[17] D. Shoenberg, *Magnetic Oscillations in Metals* (Cambridge University Press, Cambridge, England, 1984).

[18] J. M. Ziman, *Principles of the Theory of Solids* (Cambridge University Press, Cambridge, England, 1972).

[19] M. V. Kartsovnik, P. A. Kononovich, V. N. Laukhin, and I. F. Shchegolev, Pis'ma Zh. Eksp. Teor. Fiz. **48**, 498 (1988) [JETP Lett. **48**, 541 (1988)].

[20] K. Yamaji, J. Phys. Soc. Jpn. **58**, 1520 (1989).

[21] R. Yagi, Y. Iye, T. Osada, and S. Kagoshima, J. Phys. Soc. Jpn. **59**, 3069 (1990).

[22] M. V. Kartsovnik, P. D. Grigoriev, W. Biberacher, N. D. Kushch, and P. Wyder, Phys. Rev. Lett. **89**, 126802 (2002).

[23] P. D. Grigoriev, Phys. Rev. B **67**, 144401 (2003).

[24] P. D. Grigoriev, M. V. Kartsovnik, W. Biberacher, N. D. Kushch, and P. Wyder, Phys. Rev. B **65**, 060403(R) (2002).

[25] Some nonzero longitudinal magnetoresistance may appear in the τ approximation only in some special cases of complicated Fermi surface and particular directions of the magnetic field, when there are singular electron trajectories (Ref. 60).

[26] A. I. Coldea, A. F. Bangura, J. Singleton, A. Ardavan, A. Akutsu-Sato, H. Akutsu, S. S. Turner, and P. Day, Phys. Rev. B **69**, 085112 (2004).

[27] R. B. Lyubovskii, S. I. Pesotskii, A. Gilevskii, and R. N. Lyubovskaya, Zh. Eksp. Teor. Fiz. **107**, 1698 (1995) [JETP **80**, 946 (1995)].

[28] F. Zuo, X. Su, P. Zhang, J. S. Brooks, J. Wosnitza, J. A. Schlueter, Jack M. Williams, P. G. Nixon, R. W. Winter, and G. L. Gard, Phys. Rev. B **60**, 6296 (1999).

[29] J. Hagel, J. Wosnitza, C. Pfleiderer, J. A. Schlueter, J. Mohtasham, and G. L. Gard, Phys. Rev. B **68**, 104504 (2003).

[30] J. Wosnitza, J. Low Temp. Phys. **146**, 641 (2007).

[31] M. V. Kartsovnik, P. D. Grigoriev, W. Biberacher, and N. D. Kushch, Phys. Rev. B **79**, 165120 (2009).

[32] W. Kang, Y. J. Jo, D. Y. Noh, K. I. Son, and Ok-Hee Chung, Phys. Rev. B **80**, 155102 (2009).

[33] J. Wosnitza, J. Hagel, J. S. Qualls, J. S. Brooks, E. Balthes, D. Schweitzer, J. A. Schlueter, U. Geiser, J. Mohtasham, R. W. Winter, and G. L. Gard, Phys. Rev. B **65**, 180506(R) (2002).

[34] V. M. Gvozdikov, Phys. Rev. B **76**, 235125 (2007).

[35] Urban Lundin and Ross H. McKenzie, Phys. Rev. B **68**, 081101(R) (2003).

[36] A. F. Ho and A. J. Schofield, Phys. Rev. B **71**, 045101 (2005).

[37] P. D. Grigoriev, Phys. Rev. B **83**, 245129 (2011).

[38] P. D. Grigoriev, JETP Lett. **94**, 47 (2011).

[39] P. D. Grigoriev, Fiz. Nizk. Temp. **37**, 930 (2011) [Low Temp. Phys. **37**, 738 (2011)].

[40] P. D. Grigoriev, M. V. Kartsovnik, and W. Biberacher, Phys. Rev. B **86**, 165125 (2012).

[41] The square-root transverse in-plane MR $R_{xx} \propto \sqrt{B_z}$ was obtained in graphen (Ref. 61). However, this transverse MR is weaker than the classical result[16] $R_{xx} \propto B_z^2$, while for longitudinal MR the classical theory predicts no MR.

[42] P. Moses and R. H. McKenzie, Phys. Rev. B **60**, 7998 (1999).

[43] G. Mahan *Many-Particle Physics*, 2nd ed., (Plenum, New York, 1990).

[44] The MQO of the chemical potential μ can be ignored because they are usually strongly suppressed by magnetostriction, as was first shown in Ref. 62.

[45] The vertex corrections can be ignored because only short-range impurities are considered.

[46] P. D. Grigoriev, M. V. Kartsovnik, W. Biberacher, and P. Wyder, arXiv:cond-mat/0108352; P. D. Grigoriev, Ph.D. thesis,

Universität Konstanz, Konstanz, 2002, http://nbn-resolving.de/urn:nbn:de:bsz:352-opus-9127.

[47]T. Champel and V. P. Mineev, Phys. Rev. B **66**, 195111 (2002).

[48]V. M. Gvozdikov, Phys. Rev. B **70**, 085113 (2004).

[49]This notation N_{LL} denotes the area electron concentration on one LL. It coincides with N_{LL} in Ref. 37 and differs from the same notation in Ref. 23 by the factor d because in Ref. 23 N_{LL} denoted the volume LL degeneracy.

[50]The extra factor of 2 in Eq. (10) comes from the double spin degeneracy, included in the present study.

[51]Yasunari Kurihara, J. Phys. Soc. Jpn. **61**, 975 (1992).

[52]Bodo Huckestein, Rev. Mod. Phys. **67**, 357 (1995).

[53]L. S. Levitov and A. V. Shytov, JETP Lett. **66**, 214 (1997).

[54]P. D. Grigoriev, Physica B **407**, 1932 (2012).

[55]Tsunea Ando, J. Phys. Soc. Jpn. **36**, 1521 (1974).

[56]In the 3D case the diagrams with the intersections of impurity lines are small by the parameter $n_i/n_e \ll 1$, where n_i and n_e are the volume impurity and electron concentrations. In the 2D case in the magnetic field these crossing diagrams are not small by this parameter. However, the calculations of the DoS in Refs. 63 and 64 showed that these diagrams gave a small correction to the result of "noncrossing" approximation, they described the exponentially small tails of the DoS. In the quasi-2D case, which is intermediate between the 3D and 2D case, the diagrams with intersections of impurity lines can also be neglected.

[57]The spatial inhomogeniety of the electron density in the z direction due to the layered crystal structure also leads to some corrections in the electron self-energy, which are equivalent to additional integration over the strength of the impurity potential (Refs. 65,66).

[58]The impurity positions must not correlate, which may impose an upper limit on the impurity concentration $n_i < 1/R^3$, where R is the range of the impurity potential. For the short-range impurities with $R \sim 1/k_F$ this condition is not restrictive, being equivalent to the condition of metallic in-plane conductivity: $\tau E_F \gg \hbar$.

[59]Tsunea Ando, J. Phys. Soc. Jpn. **36**, 959 (1974).

[60]A. Y. Mal'tsev, Zh. Exp. Teor. Fiz. **112**, 1710 (1997) [JETP **85**, 934 (1997)],

[61]L. A. Falkovsky, Phys. Rev. B **75**, 033409 (2007).

[62]N. E. Alekseevskii and V. I. Nizhanovskii, Zh. Eksp. Teor. Fiz. **61**, 1051 (1985) [JETP **88**, 1771 (1985)].

[63]Tsunea Ando, J. Phys. Soc. Jpn. **37**, 622 (1974).

[64]E. Brezin and D. I. Gross, C. Itzykson. Nucl. Phys. B **235**, 24 (1984).

[65]A. M. Dyugaev, P. D. Grigor'ev, Yu. N. Ovchinnikov, JETP Lett. **78**, 148 (2003).

[66]I. S. Burmistrov and M. A. Skvortsov, JETP Lett. **78**, 156 (2003).